Mario Niebuhr | Axel Heuer

Phase measurement and far-field reconstruction on externally coupled laser diode arrays

Suggested citation referring to the original publication:
Optics express 25 (2017)
DOI http://dx.doi.org/10.1364/OE.25.014317
ISSN 1094-4087

Research Article | Vol. 25, No. 13 | 26 Jun 2017 | OPTICS EXPRESS 14317
Optics EXPRESS

Phase measurement and far-field reconstruction on externally coupled laser diode arrays

MARIO NIEBUHR* AND AXEL HEUER

University of Potsdam, Institute of Physics and Astronomy, Experimental Quantum Physics, Karl-Liebknecht-Str. 24-25, 14476 Potsdam, Germany
*mniebuhr@uni-potsdam.de

Abstract: Passive coherent combination of several discrete low power laser diodes is a promising way to overcome the issue of degrading beam quality when scaling single emitters to > 10 W output power. Such systems would be an efficient alternative to current high power sources, yet they suffer from fatal coherence loss when operated well above threshold. We present a new way to obtain detailed coherence information for laser diode arrays using a spatial light modulator to help identify the underlying decoherence processes. Reconstruction tests of the emitted far-field distribution are conducted to evaluate the performance of our setup.

OCIS codes: (120.5050) Phase measurement; (140.2010) Diode laser arrays; (140.3298) Laser beam combining.

References and links

1. P. Crump, C. Frevert, H. Hösler, F. Bugge, S. Knigge, W. Pittrof, G. Erbert and G. Tränkle, "Cryogenic ultra-high power infrared diode laser bars," Proc. SPIE **9002**, 90021I (2014).
2. M. Kanskar, T. Earles, T. J. Goodnough, E. Stiers, D. Botez and L. J. Mawst, "73% CW power conversion efficiency at 50 W from 970 nm diode laser bars," Electron. Lett. **41**(5), 245–247 (2005).
3. K. Paschke, S. Spießberger, C. Kaspari, D. Feise, C. Fiebig, G. Blume, H. Wenzel, A. Wicht and G. Erbert, "High-power distributed Bragg reflector ridge-waveguide diode laser with very small spectral linewidth," Opt. Lett. **35**(3), 402–404 (2010).
4. P. Crump, C. Frevert, F. Bugge, S. Knigge, G. Erbert, G. Tränkle, A. Pietrzak, R. Hüslewerde, M. Zorn, J. Sebastian, J. Lotz, W. Fassbender, J. Neukum, J. Körner, J. Hein and T. Töpfer, "Progress in high-energy-class diode laser pump sources," Proc. SPIE **9348**, 93480U (2015).
5. C. Fiebig, G. Blume, M. Uebernickel, D. Feise, C. Kaspari, K. Paschke, J. Fricke, H. Wenzel and G. Erbert, "High-Power DBR-Tapered Laser at 980 nm for Single-Path Second Harmonic Generation," IEEE J. Sel. Top. Quantum Electron. **15**(3), 978–983 (2009).
6. T. Y. Fan, "Laser beam combining for high-power, high-radiance sources," IEEE J. Sel. Top. Quantum Electron. **11**(3), 978–983 (2005).
7. J. Montoya, S. J. Augst, K. Creedon, J. Kansky, T. Y. Fan and A. Sanchez-Rubio, "External cavity beam combining of 21 semiconductor lasers using SPGD," Appl. Opt. **51**(11), 1724–1728 (2012).
8. C. J. Corcoran and F. Durville, "Passive coherent combination of a diode laser array with 35 elements," Opt. Express **22**(7), 8402–8425 (2014).
9. C. K. Hitzenberger, M. Danner, W. Drexler and A. F. Fercher, "Measurement of the spatial coherence of superluminescent diodes," J. Mod. Opt. **46**(12), 1763–1774 (1999).
10. N. W. Carlson, V. J. Masin, M. Lurie, B. Goldstein and G. A. Evans, "Measurement of the coherence of a single-mode phase-locked diode laser array," Appl. Phys. Lett. **51**(9), 643–645 (1987).
11. Y. Mejía and A. I. González, "Measuring spatial coherence by using a mask with multiple apertures," Opt. Commun. **273**(2), 428–434 (2007).
12. H. S. Partanen, S. C. Peterhänsel, C. Pruss, W. Osten, J. Tervo and J. Turunen, "Broad Area Laser Diode Coherence Measurement and Modeling," 7th International Workshop on Advanced Optical Imaging and Metrology, 879–882 (2014).
13. M. Niebuhr, C. Zink, A. Jechow, A. Heuer, L. B. Glebov and R. Menzel, "Mode stabilization of a laterally structured broad area diode laser using an external volume Bragg grating," Opt. Express **23**(9), 12394–12400 (2015).
14. J. K. Butler, D. E. Ackley and D. Botez, "Coupled-mode analysis of phase-locked injection laser arrays," Appl. Phys. Lett. **44**(3), 293–295 (1984).
15. P. P. Baveja, A. M. Kaplan, D. N. Maywar and G. P. Agrawal, "Pulse amplification in semiconductor optical amplifiers with ultrafast gain-recovery times," Proc. SPIE **7598**, 759817 (2010).
16. G. P. Agrawal and C. M. Bowden, "Concept of linewidth enhancement factor in semiconductor lasers: its usefulness and limitations," IEEE Photonics Technol. Lett. **5**(6), 640–642 (1993).

#291374 https://doi.org/10.1364/OE.25.014317
Journal © 2017 Received 27 Mar 2017; revised 5 May 2017; accepted 10 May 2017; published 14 Jun 2017

Optics EXPRESS

1. Introduction

Laser diodes (LDs) allow for the most efficient laser light sources presented up to date [1, 2]. Their high (electro-)optic conversion efficiencies in combination with a typically small footprint would make them an ideal competitor to established but comparatively bulky and inefficient high power systems. Nevertheless, upper limits to the feasible dimensions of LDs limit to either a good beam quality but moderate power [3] or vice versa [4]. While hybrid concepts have been developed [5], typical applications such as laser cutting demand for much higher output powers. An apparent ansatz would be the combination of multiple low power, good beam-quality emitters [6], ideally with a coherent scheme that will retain the good single emitter beam quality scaled to the whole array width. For such systems to work, all array emitters have to maintain a time-stable phase relation.

Various active and passive coherent combination schemes have been published to support such a phase stability [7, 8]. Especially passive setups are of interest due to the lack of necessary additional components and electronics. Unfortunately, current LD arrays and similar concepts tend to de-phase in the interesting regime of high pump/output powers even when exposed to external seed or self-feedback. It is therefore important to investigate and identify the fundamental mechanics of this de-phasing process. This can be done with measurements of the inter-emitter phase and coherence, for example based on a Mach-Zehnder interferometer [9] or interference after a double-slit like aperture [10, 11].

Here we want to introduce a new concept based on the work of Partanen et al. [12]. Instead of broad-area LDs with a continuous emitter surface, we want to investigate the characteristics of monolithic LD arrays with several discrete emitters. A spatial light modulator (SLM) is used to select the beams of only two emitters at a time. This 'double-slit' on the SLM can be easily configured to accommodate different LD arrays and measurement demands. Relative emitter phases and coherence information are extracted from the resulting interference pattern captured with e.g. a CMOS camera. We are able to provide adequate reconstructions of the emitted far-field from these measurements. Moreover, very fast acquisition rates are possible, limited only by the camera shutter, to identify characteristic timescales in the de-phasing process.

2. Principle and experimental setup

Emitter Selection: We use a phase-only spatial light modulator from HoloEye Photonics in combination with a polarizer as sketched in Fig. 1(a) as a flexible amplitude modulator to solely use light of two selected emitters for the following double-slit experiment. An additional vertical phase-grating is superimposed on the SLM to obtain an interference signal from higher diffraction orders free of any reflection background.

Relative Emitter-Phase and -Coherence: The far-field intensity distribution I from the interference of two (partially) coherent sources shown in Eq. (1) can be described as the combination of a diffraction envelope due to the slit geometry and an interference term. I_1, I_2 denote the corresponding intensities from each slit, α is the far-field emission angle and the mutual coherence function γ_{12} accounts for possible incoherent background:

$$I = \underbrace{\left(\operatorname{sinc}\frac{k \cdot d_{slit} \cdot \sin\alpha}{2}\right)^2}_{\text{diffr. envelope}} \times \underbrace{\left(I_1 + I_2 + 2\sqrt{I_1 I_2}\gamma_{12}\cos\frac{k \cdot d_{dist} \cdot \sin\alpha + \Phi}{2}\right)}_{\text{interference}} \tag{1}$$

A wave front that passes both slits simultaneously, that is with the same phase, will result in an overlap of the intensity maximum of the diffraction envelope and the interference pattern in the far-field regime as depicted in Fig. 1(b) in blue. A phase shift in the wave front from one slit compared to the second one will move the interference modulation within the diffraction envelope (red, green). It is therefore possible to obtain the phase difference between two sources,

Optics EXPRESS

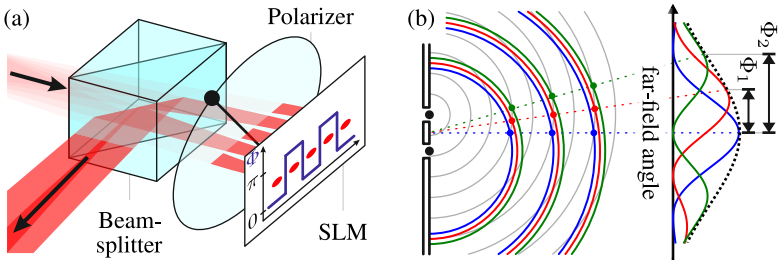

Fig. 1. (a) Schematic diagram of the polarizer and SLM combination which allows for the observation of the superposition of only 2 emitters. (b): Resulting far-field of two Huygens emitters as a simple double slit modell for phase differences of 0 (blue), $\pi/2$ (red) respectively π (green).

such as our LD array emitters, by fitting and extracting the Φ term in Eq. (1). Furthermore, one can determine the coherence γ from the visibility contrast V via Eq. eq2 (see [10]).

$$V = \frac{I_{max} - I_{min}}{I_{max} + I_{min}} = |\gamma_{12}| \frac{2\sqrt{I_1 I_2}}{I_1 + I_2} \tag{2}$$

Measurement Setup: A layout of the experimental setup is shown in Fig. 2(a). Two cylindrical lenses form a telescope to create a magnified image of the LD front-facet on the SLM in the lateral direction. The SLM, polarizer and beam-splitter select and redirect light from two emitters towards a lens + CMOS camera combination to capture the interference far-field. A second CMOS camera is used to check the LD near-field. A variable amount of neutral density filters at two positions ensures a constant camera exposure time of about 1 ms. A measurement consists of two parts. First, a single slit is moved across the SLM to obtain both the relative intensity of the array emitter images in the SLM plane as well as their position in SLM coordinates. Second, a double-slit with appropriate slit width and distance is placed in suitable positions given by step one. A python script generates the slit patterns fed to the SLM and controls the image capture process.

LD Array and External Resonator: The exemplary LD array investigated in the scope of this work is a GaAs based device emitting around a central wavelength of $\lambda_C = 980\,\text{nm}$ and comprises 9 Gaussian like emitters each 10 µm apart with a fill factor of 0.5. The array is wavelength stabilized and operated with self-induced feedback using a reflective diffraction grating similar to a setup demonstrated recently [13]. By tilting this grating around an axis parallel to the substrate plane we can adjust the central operating wavelength. Perpendicular rotation of the grating allows for emission angle selective feedback and can be used to select so called 'supermodes' [14] through their characteristic emission distribution which we will use to test our setup.

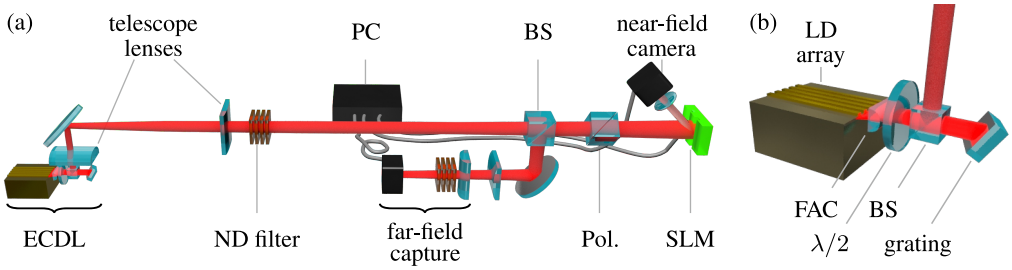

Fig. 2. (a) Rendered layout of the experimental setup. (b) Close-up of the external cavity laser-diode arrangement.

Optics EXPRESS

A short focal length cylindrical lens (FAC) collimates the beam along the fast diverging vertical axis. An additional $\lambda/2$ plate rotates the plane of the linearly polarized light as emitted by the LD array for optimal diffraction efficiency at the grating. Additionally, we use a polarizing beam-splitter cube situated within the external resonator to extract about 5 % of the circulating light toward the measurement setup, also allowing for a quick exchange of the feedback element behind the cube to e.g. a mirror or volume Bragg for further investigations. A sketch of the resonator assembly is shown in Fig. 2(b).

3. Results

Discrete LD arrays such as used here will only support a limited number of lateral eigen- or 'supermodes', resp. a corresponding superposition, because of the series of gain and loss sections in the array structure. Each supermode exhibits unique phase relations between emitters across the array and a characteristic far-field distribution [14]. By adjusting the tilt of the feedback grating to an angle of one of the main supermode lobes, we can support one and suppress the rest. We opted to tune the resonator to the supermodes which show an easily identified phase difference of 0 (inphase mode) respectively π (antiphase mode) between *all* neighboring emitters and check the phase differences to see if our setup produces similar values.

Phase Measurement: Figs. 3(a) and 3(b) show the corresponding measured nearest neighbor emitter phase differences. Additionally, data obtained when operating without external feedback (free-running) is shown in Fig. 3(c) for comparison. The phase differences for both the inphase as well as the antiphase supermode are uniformly close to the expected values. The curve from the antiphase mode shows a noticeable bend toward the array edges. Values for the free-running

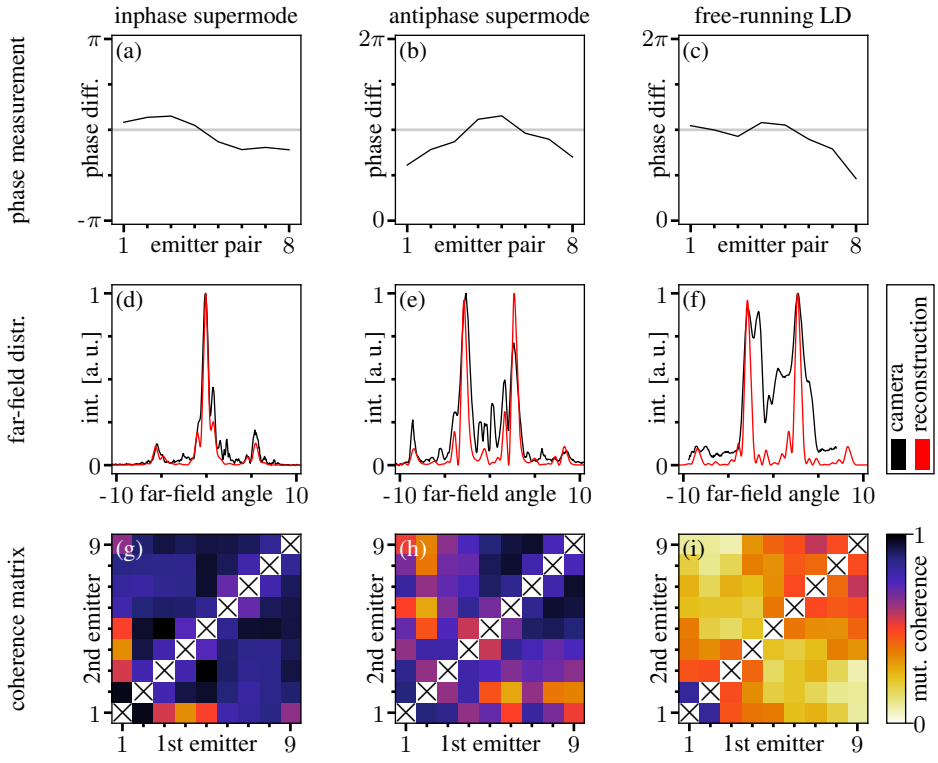

Fig. 3. Results for the inphase (left), antiphase (middle) and free-running (right) resonator system at $I_{pump} = 1.25 \cdot I_{thr}$. Upper row: phase measurement; middle row: far-field reconstruction test; lower row: coherence matrix (× indicates unmeasured values).

Optics EXPRESS

case resemble an antiphase supermode, too, albeit with a stronger drop toward one edge.

Far-Field Reconstruction: The array's far-field intensity distribution was reconstructed from the measured phase relations and emitter intensities as a form of sanity check. Nine Gaussian emitters with corresponding parameters are added up, yielding the far-field from a comparable, fully coherent array after conducting fourier transformation. Figs. 3(d)-3(f) show a comparison with the directly determined far-field distribution. We find good agreement between the measured and reconstructed curves for the inphase supermode. Besides the primary interference peaks at emission angles of $-5.5°$, $0°$ and $+5.5°$, several other features can be found in both curves at identical angles and with similar intensities. Agreement for the antiphase far-field is good as well, albeit with more dynamics in the direct measurement and some background around an emission angle of $0°$. The far-field for the free-running LD is similar to an antiphase supermode with broad background. It differs significantly from the theoretical reconstruction due to low array coherence as discussed in the next paragraph, a feature not included in the calculations.

Coherence Mapping: The visibility contrast V from phase measurement pictures can be used to obtain a spatial coherence matrix of the LD array according to Eq. (2). Graphs for the three array modes are shown in Figs. 3(g)-3(h). In the inphase case, mutual coherence is high and uniform across the whole array. Locking of one outermost emitter appears to be low. Coherence values for the antiphase case are generally lower. Only a part of the array, five to six emitters as seen in the upper right, features good locking. Values along the secondary diagonal (nearest neighbors) are lower compared to tertiary diagonal elements (second neighbors) in both cases. The coherence map for the free-running setup shows very low values and noticeable variation across the array. Two blocks with higher coherence can be seen (emitters one and two resp. emitters five through nine) with a drop in the middle of the array.

4. Discussion

A single phase measurement currently takes about 1 s, or half a minute for a complete coherence matrix of our 9 emitter LD array. We should be able to reduce the primarily readout overhead in the next iteration and reach a value close to the typical frame time of CMOS cameras ($\approx$ 10 ms). While this will already yield a quick and versatile tool for array characterization, we are following several ideas to further increase the time resolution. As the SLM does not limit the camera frame rate once a double-slit pattern is loaded, acquisition speed can be increased considerably e.g. by sweeping the interference pattern across a camera sensor ($<$ ms) or even projecting the interference pattern over a suitable arrangement of fast photo diodes ($<$ µs). This would allow us to identify the origin of de-phasing mechanisms inside the LD itself due to their characteristic time-scale (see e.g. [15, 16]) and likely compile a set of propositions for better array geometries. On the other hand, acquisition speed for different emitter combinations is limited by the SLM refresh rate of 60 Hz. While we used one double-slit at a time, several emitter interference patterns can be obtained simultaneously by feeding the SLM with multiple double-slit combinations. Each pair would have to be superimposed with a vertical grating of different period to be separable via

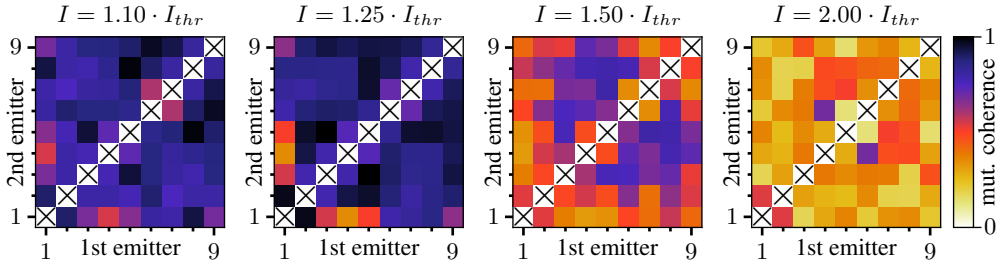

Fig. 4. Coherence matrices for the LD array operating in the *inphase* supermode at four different pump currents.

Optics EXPRESS

the corresponding diffraction angle.

We additionally observed two notable effects during our tests. First, we could witness the typical de-phasing at increasing pump powers. Corresponding coherence matrices taken with the resonator adjusted to the inphase mode at four different pump currents are shown in Fig. 4. Coherence values increase up to $I_{pump} = 1.25 \cdot I_{thr}$ followed by a rapid decline. Indeed, the coherence matrix for $I_{pump} = 2 \cdot I_{thr}$ is already similar to a matrix obtained with a free-running system at otherwise identical parameters, meaning feedback induced inter-emitter coupling through the external resonator becomes negligible compared to internal coupling. Also, the basic phase noise that diminishes the overall array coherence must work on a timescale smaller than the chosen exposure time of 1 ms, motivating the move to faster acquisition rates.

Second, all measured coherence matrices could be related to one of two cases. In some, values for nearest neighbor emitters (second diagonal elements) show a lower coherence than values for emitters two or more spaces apart. An examples is shown in Fig. 5(a). The others show a steady coherence decline with increasing emitter distance such as in Fig. 5(c). This behavior is especially apparent if looked upon by averaging the mutual coherence for all emitter combinations with similar spacing as done in Figs. 5(b) and 5(d). We think this is due to different effective reaches of the internal and external emitter coupling. While a single emitter internally affects nearest neighbors with fast declining (leaky wave) coupling for increasing emitter distance, effects due to self-induced feedback through the external resonator are overall weaker, because the beam expands, but simultaneously affect emitters farther away. Our system is therefore additionally suited to assess selected characteristics of the LDs, such as the quality of the internal resonator based on (anti-)reflective coatings, using a normed external resonator assembly as point of comparison.

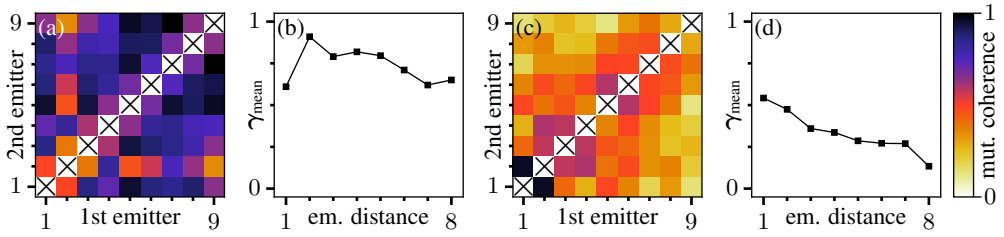

Fig. 5. Exemplary coherence matrices and averaged mutual coherence trace. (a)/(b) exhibit additional coupling through the external resonator and show reduced nearest neighbor coherence, (c)/(d) show data from a feedback free measurements (internal coupling only).

5. Conclusion

We presented a concept to quickly determine inter-emitter phase differences and mutual coherence in typical LD arrays that is scalable in the number of arrays as well as array emitters. We generally find good agreement between theory and measurement in our test runs if the LD array emits in a defined supermode with high overall array coherence. The, in some cases more noticeable, deviations from our ideally coherent calculations coincide with lower and nonuniform coherence values observed for e.g. the antiphase supermode and thereby do not denounce the functionality of this setup. Furthermore, we could already identify a competition between two coupling mechanisms that reduces the overall array coherence and we were able to keep track of a fast loss of array coherence for increasing pump current as frequently reported in literature.

Funding

Deutsche Forschungsgemeinschaft; Open Access Publication Fund of University of Potsdam.

Acknowledgments

We would like to thank Tino Fremberg and Dennis Mayer for their assistance in this project as well as PBC lasers Berlin for supplying the LD array and Markus Gühr for fruitful discussions.